POLYPROPYLENE COMPOSITES REINFORCED WITH RICE STRAW MICRO/NANO FIBRILS ISOLATED BY HIGH INTENSITY ULTRASONICATION

Yan Wu,[a,b] Ding-Guo Zhou,*[,a] Si-Qun Wang,[a,b] and Yang Zhang [a]

Rice straw (*Oryza sativa L.*) pulp was treated by high intensity ultrasonication to make fibrils. The rice straw fibril (RSF) material was used as reinforcement in an RSF/polypropylene (PP) composite. The influences of RSF and coupling agent (MAPP) contents on tensile properties of the composite were tested. The results showed that when RSF loading was 5%, the tensile strength rose to a maximum value of 31.7 MPa. With increasing fibril loading the tensile modulus increased first, then decreased. However, the elongation at break decreased with increasing fibril loading. There was no significant influence of MAPP content on tensile strength and elongation at break of PP and RSF/PP composite. When MAPP content was 4%, the tensile modulus of PP and RSF/PP composite all showed maximum values.

INTRODUCTION

Composites reinforced with natural fibers are those in which the thermoplastic component exists in a continuous matrix and the lignocellulosic component serves as reinforcing filler. The great majority of reinforced thermoplastic composites available commercially use inorganic materials as their reinforcing fillers, e.g. glass, clays, and minerals. These materials are heavy, abrasive to processing equipment, and non-renewable. In recent years, lignocellulosic fillers used to reinforce thermoplastics, such as polypropylene (PP) and polyethylene (PE) have expanded due to their strength, low density, relatively high aspect ratio, and environmental benefits. Lignocellulosic materials such as wood fiber, wood flour, cellulose fiber, flax, and hemp have been given increased attention by polymer manufactures (Bataille et al. 1989; Leaversuch et al. 1999; Sherman et al. 1999; Karnani et al. 1997).

Rice straw is an agricultural byproduct and it is easy to obtain. The rice straw has the merits of low density, greatly reduced wear of the processing machinery, and a relatively reactive surface. In addition to these attractive properties, it is abundant and has a low price. Moreover, the recovery of energy and resources by combustion of cellulose-filled composites is easier in comparison with inorganic filler systems. Nevertheless, such fibers are used only to a limited extent in industrial practice, which may be explained by difficulties in achieving acceptable dispersion levels (Helbert 1996). The nanofibril is

deemed to be the minimum cellulosic structure unit, which is made up of cellulose molecular chains having high stiffness and modulus, yielding a structure having lower density and better mechanical properties. Moreover, the micro/nano fibrils isolated from natural fibers have much higher mechanical properties. Sakurada et al. (1962) reported that the cellulose crystal regions are a bundle of stretched cellulose chain molecules with Young's modulus of 150 GPa and strength in the order of 10 GPa. The elastic modulus of cellulose fibril with a diameter of about 170 nm was evaluated to be 93 GPa using AFM (Cheng et al. 2008). Therefore it can partly take the place of glass fiber, carbon fiber, and other man-made fibers as the filler to compound biodegradable nancomposites (Cheng et al. 2007; Zimmermann et al. 2004).

       Cellulose is hydrophilic due to the hydroxyl groups in its chemical structure and therefore it is incompatible with the hydrophobic thermoplastic materials. In order to obtain high performance wood polymer composite, surface modification is needed, which can significantly improve the mechanical properties of the resulting product (Gauthier et al. 1998). Generally the esterification can supply the non-polar chemical function group, which can improve the interface compatibility between cellulose fiber and polymer (Felix et al. 1993; Milewski et al. 1987; Qin 1997; Sanadi 1997).

       High intensity ultrasonication, as a novel method for fibril isolation, was used to treat several cellulose materials to generate small fibrils in nano and micro scales (Cheng et al. 2009). It can produce very strong mechanical oscillating power, so the separation of cellulose microfibril from cellulose may be possible by the action of hydrodynamic forces of ultrasound. They are widely used in many processes, especially in emulsification, catalysis, homogenization, disaggregation, scission, and dispersion (Anonymous 2001 and 2002).

       The objective of this work is to use rice straw pulp fiber to prepare environmentally friendly rice straw fibrils by high intensity ultrasonication (HIUS) and to evaluate rice straw fibrils as a novel reinforcing material to compound rice straw fibril (RSF)/polypropylene (PP) composite. The mechanical properties were measured by tensile testing. Scanning electron microscopy (SEM) was used to investigate the morphology characteristic of fracture of RSF/PP composite after tensile testing. The interface compatibility was investigated by Fourier transform infrared spectroscopy (FTIR).

EXPERIMENTAL

Materials

       Rice straw pulp fibers were kindly supplied by Taonan Paper and Pulp Company, Jilin, China. The fibers were cut to pass a screen (room temperature and relative humidity of 30%) with holes of 1 mm in diameter by a Wiley mill before treatment as shown in Fig. 1. The isotactic polypropylene (iPP) used in this study was supplied by FiberVisions, Georgia, USA, in the form of homopolymer pellets with a melt flow index of 35g/10 min (230 ºC, 160 g) and a density of 0.91 g cm^{-3}. The maleated polypropylene (MAPP) was used as compatibilizing agent and Epolene G-3003 P has an acid number of 6 and a molecular mass of 125 722.
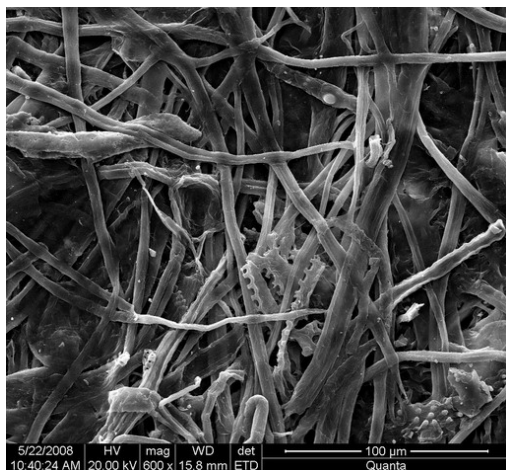
Fig. 1. SEM image of rice straw pulp fiber (mag. 600×)

Fibril Isolation

The milled rice straw pulp fibers were soaked in distilled water for more than 24 h, which tends to make the fibers intenerate and easy split, and then treated by high intensity ultrasonication (Sonics & Materials. INC, CT, 20kHz, Model 1500 W) for 30 min with 80% power level. The fibers were immersed in 60 ml of distilled water in a 100-ml beaker. The fiber concentration was 1% W/W. After ultrasonication treatment, the obtained RSF aqua compound was kept frozen. The laser diameter instrument (Winner 2005, Qingdao, China) was used to investigate the diameter distribution after HIUS treatment.

Freeze Drying

In order to avoid the aggregation of isolated RSF, the frozen RSF aqua compound was freeze-dry at Food Science, the University of Tennessee, Knoxville, TN, USA. The conditions of freeze drier (Virtis Genesis 12 EL) were -20 ℃ to + 20 ℃ over 4 days in 5 ℃ increments.

Compounding

The freeze-dried RSF was milled by a food processor and kept in a dessicator. The RSF/ PP composite was made by blending PP pellets with 1~6% MAPP (ratio of PP weight, wt%) and 2~11% RSF (ratio of total weight, wt%). All materials were then fed into a Haake Mini-Lab twin-screw extruder (Thermo Electron Corp., Hamburg, Germany). The blends were processed for 10 min, 20 min, and 30 min at 50 rpm and 180 ℃, 190 ℃, and 200 ℃ using a counter-rotating screw configuration, respectively. The RSF/PP composite was then extruded through a 2.5 mm cylindrical die. The extruder strands were granulated and hot pressed at a temperature of 175 ℃ and a pressure of 5 MPa for 10 min. The obtained sheets with nominal thickness of 270 μm were conditioned at 23 ± 2 ℃ and $50 \pm 5\%$ relative humidity for not less than 40 h prior to tensile testing in accordance with ASTM D 618 Standard Practice for Conditioning Plastics for Testing (ASTM D 618-00).

Tensile Test

The tensile measurements were conducted on an Instron testing machine (Model 5567) with a length of 20 mm between the top and bottom clamps, a crosshead speed of 1 mm/min, and a load cell of 30 kN (Cheng et al. 2007). The specimens were cut to dogbone shapes with width of 5 mm for the narrow portion and total length of 40 mm. A schematic illustration of tensile specimen is shown in Fig. 2. Eight specimens were tested for each composition according to the ASTM D 882 standard test method for tensile properties of thin plastic sheeting (ASTM D 882 - 02). Multiple comparisons by the Statistical Analysis System JMP version 6.0.2 software (SAS Institute, Cary, NC, USA) (t Tests (LSD)) were used to detect the overall significant differences of the influences on the tensile strength and elastic modulus of composites ($\alpha = 0.05$).
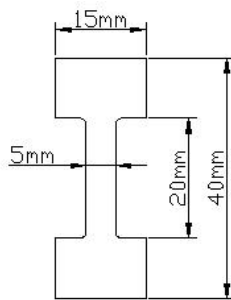
Fig. 2. Schematic illustration of tensile specimen

Morphological Characteristics

The fractured surfaces of composites after tensile testing were investigated by a scanning electron microscopy (SEM, LEO 1525). The voltages were 5-10 kV, and various magnification levels were used to obtain images.

FTIR Testing

The interfacial compatibility of samples was tested by FTIR accompanied by ATR. The sample scanning times was 64, the ratio of differentiate was 8.000, sampling plus was 2.0, the speed of moving lens was 0.6329, diaphragm was 100.00, and wave range was 4000~400cm^{-1}.

RESULTS AND DISCCUSION

Effect of Different RSF Loadings on RSF/PP Composite Tensile Properties

The tensile strength of RSF/PP composites with different fibril loadings is shown in Fig. 3. As the reference, the tensile strength of PP/MAPP polymer was also tested. Results showing the effect of MAPP on the properties of composites can be found in Figs. 8, 9, and 11. The tensile strength at 5% RSF loading was up to the maximum value, 31.7 MPa, which was a little higher than the value of PP/MAPP polymer, 30.8 MPa. With increasing the fibril loadings, the tensile strength appeared to decrease, but the trend was not distinct ($R^2 = 0.23$). The tensile strength of RSF/PP composite was lower than PP/MAPP polymer, except for the loading of 5% of RSF.
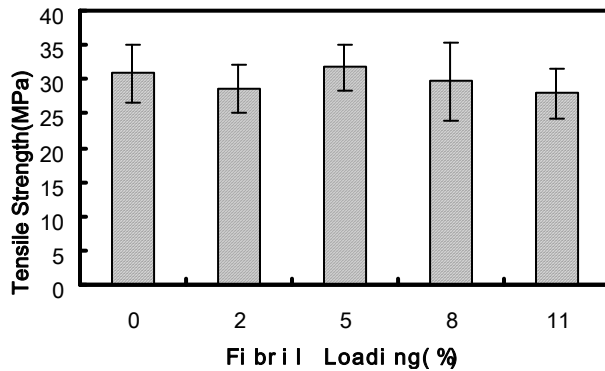
Fig. 3. Tensile strength of different fibril loading at the extruder condition of 200ºC, 10 min

The SEM images showed that there were some large fibril aggregates in the RSF/PP composite at the loading of 11%, and gaps between fibril aggregates and polymer were also seen (Figs. 4 a and b).
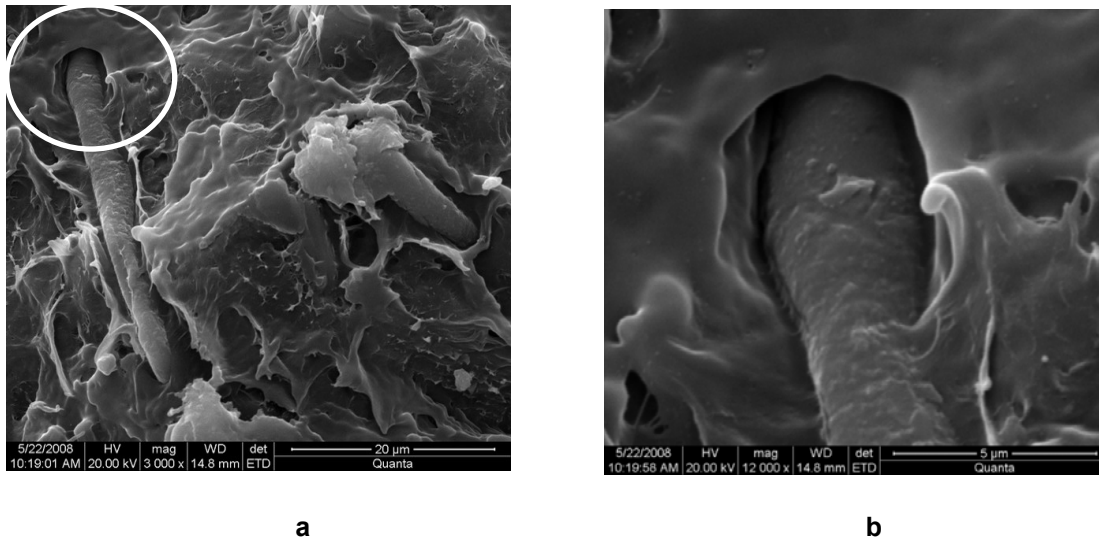

a   b

Fig. 4. Fracture cross section SEM images of RSF/PP composite after tensile test (a. mag. 3000×; b. 12000×)

Two main processes may explain the existence of gaps: One is the effect of the ultrasonication treatment, which could not isolate all the fibers to the nano or micro size fibrils. Support for this idea is provided by the analysis of the distribution of RSF diameters (Fig. 5). The distribution of diameters of RSF ranged from 0.1 μm to 80 μm by HIUS treatment. The percentage was 6.3% of RSF, the diameters of which were less than 500 nm; almost 90 percent of the RSF were distributed between 7.0 μm and 80 μm; the average diameter was 41 μm.
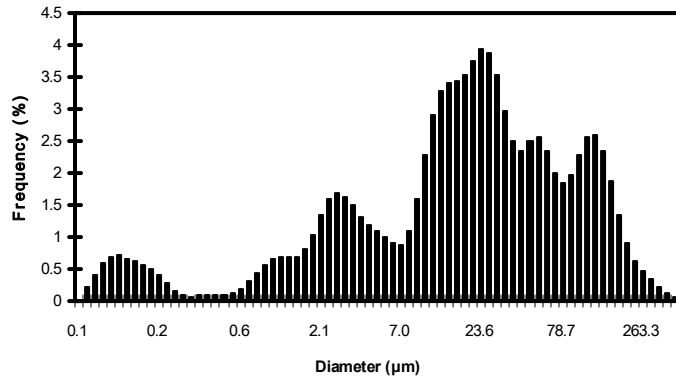
Fig. 5. Distribution of RSF diameters treated by HIUS

Another likely explanation is that the effect was due to the freeze drying treatment, during which the water was transformed from ice to water vapor, while there were still some fibrils bundled together because of large of hydrophilic hydroxyl groups. These factors may have produced the difficulties of uneven distribution of RSF in the matrix, which also resulted in the lower tensile strength of RSF/PP composite than PP/MAPP polymer. Therefore, it is very important for nano and micro size fillers to be suitably purified, and appropriate steps should be taken for surface modification and optimization of the procedure of HUIS treatment in future work.

Figure 6 shows the elastic modulus of RSF/PP composite with different fibril loadings. The values were higher in RSF/PP composite than in PP/MAPP polymer. The fibril loadings from 2% to 8%, the elastic modulus increased significantly ($R^2 = 0.70$). The maximum was 1621 MPa at the 8% of RSF, which was 17% higher than the value of PP/MAPP polymer. From 8% to 11% of RSF, the elastic modulus decreased.
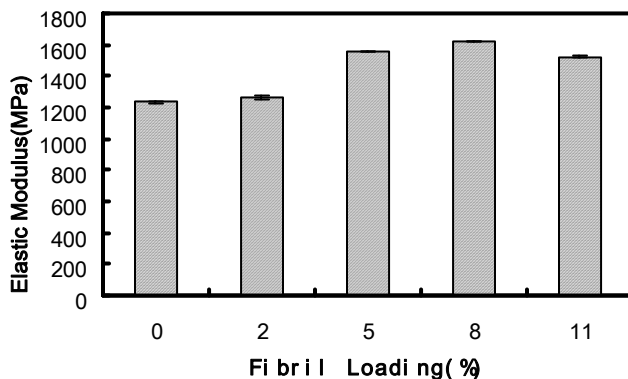

Fig. 6. Elastic modulus of different fibril loading at the extruder condition of 200ºC, 10 min

By adding the RSF, the rigidity of matrix increased, but the regular tropism of molecule chain was restricted, blocking its ability to flow and reducing its ductility. This also was exhibited by the fact that with increasing RSF loadings the elongation at break decreased ($R^2 = 0.89$) as shown in Fig. 7.
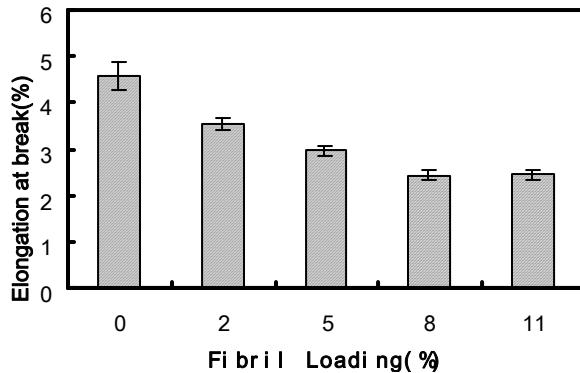

Fig. 7. Elongation of different fibril loading at the extruder condition of 200ºC, 10 min

Effect of MAPP Content on RSF/PP Composite Tensile Properties

Figure 8 shows the effect of coupling agent MAPP on RSF/PP composite tensile properties. There were no significant changes of tensile strength in PP/MAPP polymer and RSF/PP composite with increasing MAPP content from 1% to 6%.
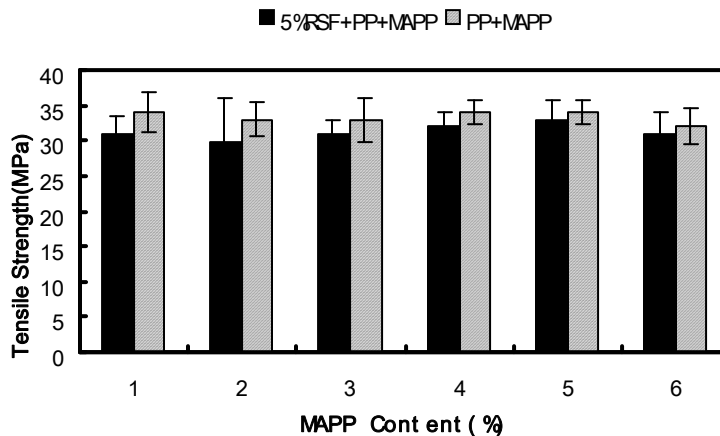

Fig. 8. Tensile strength of different MAPP content at the extruder condition of 200ºC, 10 min

The elastic moduli of RSF/PP composite and PP/MAPP polymer both showed maximum values at the 4% of MAPP, which were 1509 Mpa and 1341 Mpa, respectively (Fig. 9).
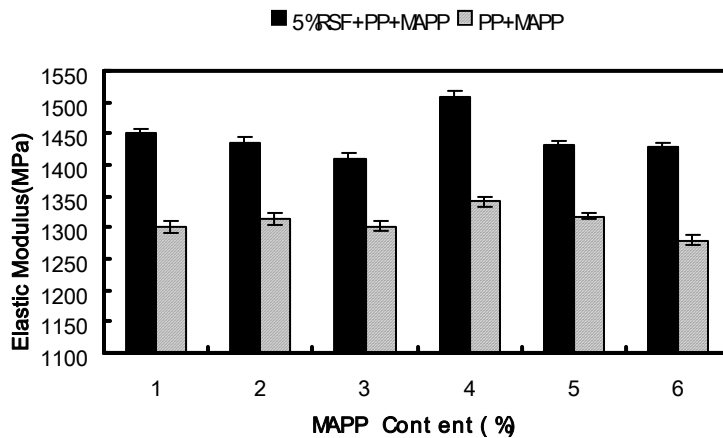
Fig. 9. Elastic modulus of different MAPP content at the extruder condition of 200ºC, 10 min

Figure 10 shows the FTIR spectra of PP, RSF/PP composite, and RSF, arranged from top to bottom. When adding MAPP and RSF into a PP matrix, the FTIR spectra showed prodigious changes. CH_3 deformation of asymmetry stretching and CH_2 symmetry stretching moved to higher wavenumbers. Moreover, the frequency of CH_3 symmetry deformation decreased (1374 cm^{-1} to 1372 cm^{-1}). The existence of C-O-C stretching at 1224 cm^{-1}, 1074 cm^{-1}, and 1028 cm^{-1} indicated that PP and RSF did not change with the addition of MAPP.
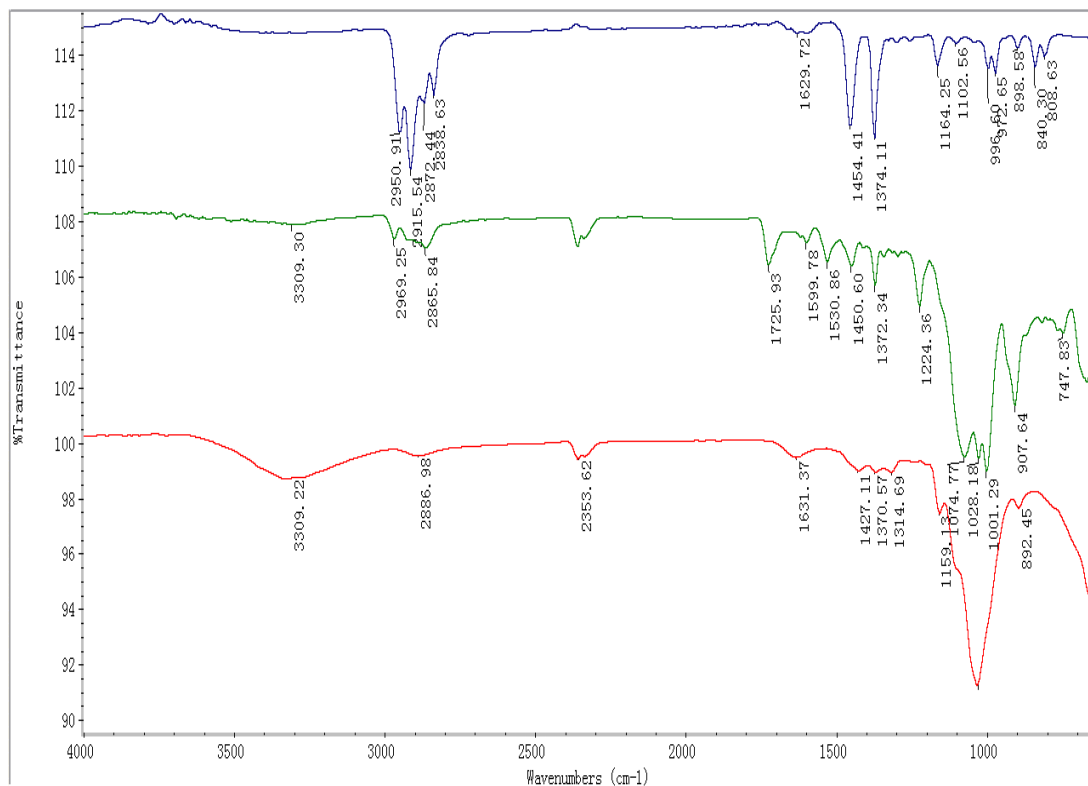

Fig.10. FTIR curves of PP, RSF/PP composite and RSF

The addition of MAPP improved the compatibility of interface between RSF and matrix, which increased the rigidity of composite. However, there was no distinct influence on the elongation at break of both composite and PP/MAPP polymer, as shown in Fig. 11.
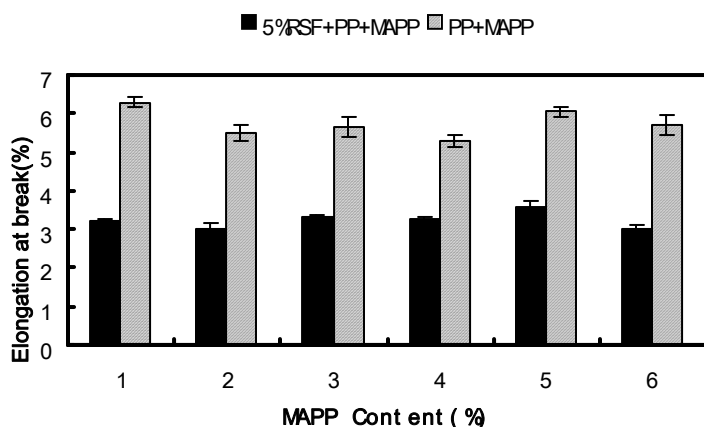

Fig. 11. Elongation at break of different MAPP content at the extruder condition of 200ºC, 10 min

CONCLUSIONS

The rice straw fibril (RSF) derived from high intensity ultrasonication (HIUS) treatment could be used effectively as a filler to reinforce PP/MAPP polymer. The tensile strength rose to a maximum value at 5% content of RSF, the elastic modulus increased with increasing RSF, and the maximum value was 8%. The elongation at break decreased with increasing RSF. When MAPP was up to 4%, the RSF/PP composite and PP/MAPP polymer both showed maximum values. However, there was no significant influence of adding MAPP on tensile strength and elongation at break of RSF/PP composite and PP/MAPP polymer. The purity and distribution of RSF should be improved and the characteristics of the interface of RSF/PP should be further investigated.

ACKNOWLEDGMENTS

REFERENCES CITED

Anonymous (2001). "Ultrasonic treatment technology description,"
http://www.nemw.org/Balsurv3_US.htm.

Anonymous (2002). "What are ULTRASONICS and ULRASONIC PROCESSING?"
Sonic & Materials, Inc.

ASTM D 618. "Standard practice for conditioning plastics for testing," (ASTM D 618-00).

ASTM D 882. "Standard test method for tensile properties of thin plastic sheeting,"
(1989; D 882 - 02).

Bataille, P., Ricard, L., and Sapieha, S. (1989). "Effects of cellulose fibers in
polypropylene composites," *Polym. Compos*. 10, 103.

Cheng, Q. Z., and Wang, S. Q. (2007). "Current research on the nanocomposite
reinforced with natural lignocellulosic micro/nano fibrils," *Industry of Forest
Products* 34(3), 3-7.

Cheng, Q. Z., Wang, S. Q., Harper, D. Y., Wang, J., and Liu, Y. (2008). "Elastic modulus
of single cellulose fibrils evaluated by atomic force microscopy," Proceedings of IA
WPS 2008, Harbin China, September 27-29, 531-533.

Cheng, Q. Z., and Wang, S. Q. (2009). "A novel process to isolate fibrils from cellulose
fibers by high-intensity ultrasonication. Part 2. Fibril characterization," *Journal of
Applied Polymer Science*. (in press).

Felix, J. M., Gatenholm, P., and Schreiber, H. P. (1993). "Controlled interactions in
cellulose-polymer composites. I. Effect on mechanical properties," *Polym. Compos*.
14, 449.

Gauthier, R., Joly, C., and Coupas, A. C. (1998). "Interfaces in polyolefin/cellulosic fiber
composites: Chemical coupling, morphology, correlation with adhesion and aging in
moisture," *Polym. Compos*. 19(3), 287-290.

Helbert, W. J., Cavaillé, Y., and Dufresne, A. (1996). "Thermoplastic nanocomposites
filled with wheat straw cellulose whiskers. Part I: processing and mechanical
behavior," *Polym. Compos*. 17 (4), 604-611.

Karnani, R., Mohan, K., and Ramini, N. (1997). "Biofiber-reinforced polypropylene
composites," *Polymer Engineering and Science* 37, 476.

Leaversuch, R. D. (1999). "Fillers, fibers, and blends remake PP," *Chemical Week
Publishing*. 76, 58.

Milewski, J. V., and Harry, S. K. (1987). *Handbook of Reinforcements for Plastics*, New
York. 6-9 pp.

Qin, T. F. (1997). "The way to improve wood plastic composite interface," *Research on
World Forestry* 11 (3), 46-50.

Sakurada, I., Nukushina, Y., and Ito, T. (1962). "Experimental determination of elastic
modulus of crystalline regions in oriented polymers," *Journal of Polymer Science*
57(165), 651-660.

Sanadi, A. R., et al. (1997). "Agro-fiber thermoplastic composites," in *Paper and
Composites from Agro-bases Resources*, Rowell, R. M., Young, R. A., and Rowell, J.
K. (eds.), CRC Press, Boca Raton, Fl. 378-399 pp.

Sherman, L. M. (1999). "Natural fibers. Plastics technology," Online. Link at: http://www.plastictechnology.com/articles/199910fal.html accessed on 15.06.2003.

Zimmermann, T., Pohler, E., and Geiger, T. (2004). "Cellulose fibrils for polymer reinforcement," *Advanced Engineering Materials* 6(9), 754-761.